Remote Sensing of Environment 143 (2014) 171–179

Contents lists available at ScienceDirect

Remote Sensing of Environment

journal homepage: www.elsevier.com/locate/rse

Landsat remote sensing of forest windfall disturbance

Matthias Baumann [a,*], Mutlu Ozdogan [a], Peter T. Wolter [b], Alexander Krylov [c], Nadezda Vladimirova [c], Volker C. Radeloff [a]

[a] Department of Forest and Wildlife Ecology, University of Wisconsin-Madison, 1630 Linden Drive, Madison, WI 53706-1598, USA
[b] Department of Natural Resource Ecology and Management, Iowa State University, 339 Science Hall II, Ames, IA, 50011, USA
[c] The Transparent World, Rossolimo str. 5/22, Building 1, Moscow 119021, Russian Federation

ARTICLE INFO

Article history:
Received 4 April 2013
Received in revised form 28 December 2013
Accepted 29 December 2013
Available online 28 January 2014

Keywords:
Landsat
Windfall
Forestness Index
Disturbance Index
Tasseled Cap transformation

ABSTRACT

Knowing if a forest disturbance is caused by timber harvest or a natural event is crucial for carbon cycle assessments, econometric analyses of timber harvesting, and other research questions. However, while remote sensing of forest disturbance in general is very well developed, discerning between different types of forest disturbances remains challenging. In this work, we developed an algorithm to separate windfall disturbance from clear-cut harvesting using Landsat data. The method first extracts training data primarily based on Tasseled Cap transformed bands and histogram thresholds with minimal user input. We then used a support-vector machine classifier to separate disturbed areas into 'windfall' and 'clear-cut harvests'. We tested our algorithm in the temperate forest zone of European Russia and the southern boreal forest zone of the United States. The forest-cover change classifications were highly accurate (~90%) and windfall classification accuracies were greater than 75% in both study areas. Accuracies were generally higher for larger disturbance patches. At the Russia study site about 60% of all disturbances were caused by windfall, versus 40% at the U.S. study site. Given the similar levels of accuracy in both locations and the ease of application, the algorithm has the potential to fill a research gap in mapping wind disturbance using Landsat data in both temperate and boreal forests that are subject to frequent wind events.

1. Introduction

Forests play an important role in the global carbon cycle and the provision of ecosystem services. Information on where and to what extent forest disturbances occur globally is thus a crucial necessity (Achard et al., 2002; Bonan, 2008). Remote sensing can provide accurate and timely information regarding forest disturbance in many ecoregions at scales ranging from local to global and at many different temporal resolutions (Achard et al., 2006; Baumann et al., 2012; Hansen & DeFries, 2004; Hansen, Stehman, & Potapov, 2010; Healey, Cohen, Yang, & Krankina, 2005; Huang et al., 2010; Potapov, Hansen, Stehman, Pittman, & Turubanova, 2009; Potapov et al., 2012; Zhu, Woodcock, & Olofsson, 2012). Data from Landsat Thematic Mapper (TM) and Enhanced Thematic Mapper Plus (ETM+) instruments have been used for many of these studies because of (1) the favorable combination of spatial, spectral and temporal resolution, (2) the free availability of the data (Wulder, Masek, Cohen, Loveland, & Woodcock, 2012) and, (3) the long-term data record, which continues now thanks to the Landsat Data Continuity Mission (LDCM, Irons, Dwyer, & Barsi, 2012).

In most forest disturbance mapping studies that utilize Landsat data, the derived change products only identify areas of 'forest disturbance', but do not discriminate among different types of disturbances (e.g., Cohen, Fiorella, Gray, Helmer, & Anderson, 1998; Coppin & Bauer, 1994; Ozdogan, in press). This has already been identified as a gap in remote sensing based forest disturbance studies (e.g., Hicke et al., 2012; Kasischke et al., 2013; Masek et al., 2011; Vogelmann, Tolk, & Zhu, 2009). The lack of attribution to the type of disturbance often makes it difficult to interpret forest disturbance maps, especially when these data are used as inputs to carbon budget assessments or econometric analyses. For example, many studies that seek to understand timber harvest trends are forced to equate forest disturbance with harvesting (e.g., Chomitz & Gray, 1996; Wendland et al., 2011). As a result, natural disturbance is erroneously included in harvest estimates, which can lead to overestimation of harvested areas and dampen the significance of actual drivers of forest harvest. Inability to separate forest harvest from natural disturbances also affects studies that assess the effectiveness of protected areas in preventing logging (e.g., Hayes, 2006; Andam, Ferraro, Pfaff, Sanchez-Azofeifa, & Robalino, 2008; Wendland, Baumann, Lewis, Sieber, & Radeloff, in review). From the ecological point of view, information on the type of forest disturbance is important for biomass estimations and for the prediction of post-disturbance succession (Kasischke et al., 2013; Scheller & Mladenoff, 2004). For example, more living biomass remains in place following a windfall event, compared to a clear-cut harvest, which can hinder the establishment of early successional species (Peterson, 2000; Webb & Scanga, 2001; Rich, Frelich, Reich, & Bauer, 2010; Scheller & Mladenoff, 2004).

The most common natural disturbances affecting forests are fire, insect defoliation and windfall (FAO, 2005; FAO, 2010). While remote sensing of fire-related disturbances and insect defoliation has received

* Corresponding author. Tel.: +1 608 265 9219; fax: +1 608 262 9922.
E-mail address: mbaumann3@wisc.edu (M. Baumann).

0034-4257/$ – see front matter © 2014 Elsevier Inc. All rights reserved.
http://dx.doi.org/10.1016/j.rse.2013.12.020

considerable attention in the past (e.g., French et al., 2008; Garcia-Haro, Gilabert, & Melia, 2001; Patterson & Yool, 1998; Pereira & Setzer, 1993; Roder, Hill, Duguy, Alloza, & Vallejo, 2008; Schroeder, Wulder, Healey, & Moisen, 2011; Townsend et al., 2012; Van Wagtendonk, Root, & Key, 2004), only a handful of studies have focused on identifying and mapping windfall disturbances. In general, the existing studies can be categorized into two themes. The first category focuses on monitoring the impacts of tropical storms on forest structure using multispectral imagery or radar data (e.g. Cheung, Pan, Gu, & Wang, 2013; Negron-Juarez, Baker, Zeng, Henkel, & Chambers, 2010; Nelson, Kapos, Adams, Wilson, & Braun, 1994; Ramsey, Rangoonwala, Middleton, & Lu, 2009; Ramsey, Werle, Lu, Rangoonwala, & Suzuoki, 2009; Wang & Xu, 2010). The second area of focus is severe storm (including tornados) damage on forests of continental interiors, which are characterized by smaller affected areas but high intensity disturbances, such as the Boundary Waters Blowdown in the Greater Border Lakes Region (USA) in 1999 (Rich et al., 2010; Wolter et al., 2012). However, while these studies were successful in mapping the damage caused by each particular storm, they did not include developing a specialized, and potentially universal, method to separate wind-related change from other disturbances.

The Disturbance Index (DI, Healey et al., 2005) is an example of a universal method. The algorithm has been developed to detect areas of forest disturbance, and has been tested in a wide range of forest biomes including the Pacific Northwest (USA), the St. Petersburg and other locations in Russia, South-Sudan and Uganda and the conterminous United States (Healey et al., 2005; Masek et al., 2008; He et al., 2011; Gorsevski, Kasischke, Dempewolf, Loboda, & Grossmann, 2012; Sieber et al., 2013). One reason for the success of the DI is its use of the Tasseled Cap transformation that convert Landsat bands into brightness', 'greenness', and 'wetness' measures to describe the variations in soil background reflectance, vegetation vigor, and vegetation senescence, respectively (Crist & Kauth, 1986; Kauth & Thomas, 1976). The success of the Tasseled Cap bands in the DI across different study regions suggests that a windfall classification algorithm based on the same standardized bands might be successful as well across different regions throughout the world.

Our goal here was to develop an algorithm to distinguish windfall disturbance from forest harvests with Landsat data in two different locations. Our specific objectives were to:

1 create a map of forest and forest disturbance using established methods from the literature,
2 develop an algorithm to separate the areas of forest-disturbance into windfall disturbance and clear-cut harvests,
3 test our algorithm in two study regions, (1) the temperate zone of European Russia and (2) the southern boreal forest zone of the United States.

2. Methods

2.1. Study area

Our first study site is located in the temperate zone of European Russia (Landsat Path/Row 177/019, Fig. 1 bottom right). Temperate coniferous, broadleaf, and mixed forests dominate the landscape with Norway spruce (*Picea abies*) and Scots pine (*Pinus sylvestris*) being the most abundant coniferous species. Major deciduous species include aspen (*Populus tremula*), gray alder (*Alnus incana*), and birch (*Betula pendula*). Commercial harvests are widespread in the region, because the Russian forestry sector is growing and western forest companies are increasing their investments in mills to exploit Russia's vast timber resources (Mutanen & Toppinen, 2007). Besides commercial harvests, the region experiences frequent natural disturbance events. Specifically, the study region experienced two storms that occurred in October 2009 and July 2010 (Koroleva & Ershov, 2012), which were studied and mapped in detail by the Russian Forest Health Center (Krylov, Malahova, & V., 2012).

The second study site is located in the southern boreal forests in northern Minnesota (USA) (Landsat Path/Row 025/028, Fig. 1, bottom left). The region is characterized by a mixture of glacial lakes and wetlands. Forest species in the region include early successional species, such as jack pine (*Pinus banksiana*), red pine (*Pinus resinosa*), or aspen (*Populus tremuloides*), as well as late successional species like white cedar (*Thuja occidentalis*) or balsam fir (*Abies balsamea*) (Frelich & Reich, 1995; Rich et al., 2010). In 1999, the region experienced a large infrequent wind disturbances event, which is referred as the Boundary Waters Blowdown (or the Boundary Waters Canadian Derecho). The storm occurred between July 4th and 5th 1999 and lasted 22 h. It traveled over 2000 km at an average pace of around 95 km/h, and with wind gusts of over 160 km/h. The storm caused over 1500 km^2 of considerable forest damage (Price & Murphy, 2002), and has been a research subject in the past (Rich et al., 2010; Wolter et al., 2012).

2.2. Image pre-processing

At both locations we analyzed Landsat data from the year before and the year after the windfall event. Our temporal frames were 1998–2000 for the U.S. site and 2009–2011 for the Russia site. Imagery for both study sites were pre-processed by converting digital numbers into surface reflectance using the Landsat Ecosystem Disturbance Adaptive Processing System (LEDAPS) algorithm (Masek et al., 2006). Cloud-free images were available for both time points at the U.S. site, but not for the Russia site. Therefore, we selected images with the least amounts of clouds (hereafter called the base-image) and gap-filled them using other Landsat scenes from the same growing season (i.e., late May to August; 2009 and 2011, respectively, Table 1). Gap-filling was accomplished by first masking clouds and cloud shadows in each image using FMask (Zhu & Woodcock, 2012), applying conservative threshold values to ensure that a maximum of clouds and cloud shadows were detected. Afterwards, we filled the gaps of our base-image using all other images from the respective growing season. We ensured that images located at the edge of a growing season (i.e., late May) were chosen last to fill gaps in the base-image. We thus minimized potential influences of a late spring onset that sometimes can lead to class confusions in forest/non-forest classifications. The result was a nearly cloud-free image composite for both time points (2009 and 2011).

2.3. Forest/non-forest classification

For both study sites, we classified the pre-disturbance image (1998 for the U.S. site, and 2009 for the Russia site) into 'forest' and 'non-forest' using a training data set generated automatically using the dark object approach (Huang et al., 2008). More specifically, we searched for the peak within a local histogram of Landsat's red band (Band 3). In the absence of non-vegetated dark objects, such as water or dark soil, pixels to the left of the peak can be considered forest pixels (Huang et al., 2008). We removed non-vegetated dark objects by applying a consistency check using the globally available Moderate-Resolution Imaging Spectroradiometer (MODIS) vegetation continuous field product (VCF, Hansen et al., 2006) with a threshold value of 40%. Dark pixels passing this consistency check were then collected within a group of confident forest samples and used to calculate the Integrated Forestness Index (IFI):

$$IFI = \sqrt{\frac{1}{NB}\sum_{i=1}^{NB}\left(\frac{b_{pi}-\overline{b_i}}{SD_i}\right)^2} \quad (1)$$

where $\overline{b_i}$ and SD_i are the mean and standard deviation of the candidate forest pixels within that image for band i, b_{pi} is the spectral value for pixel p in band i, and NB is the number of bands (Huang et al., 2008).

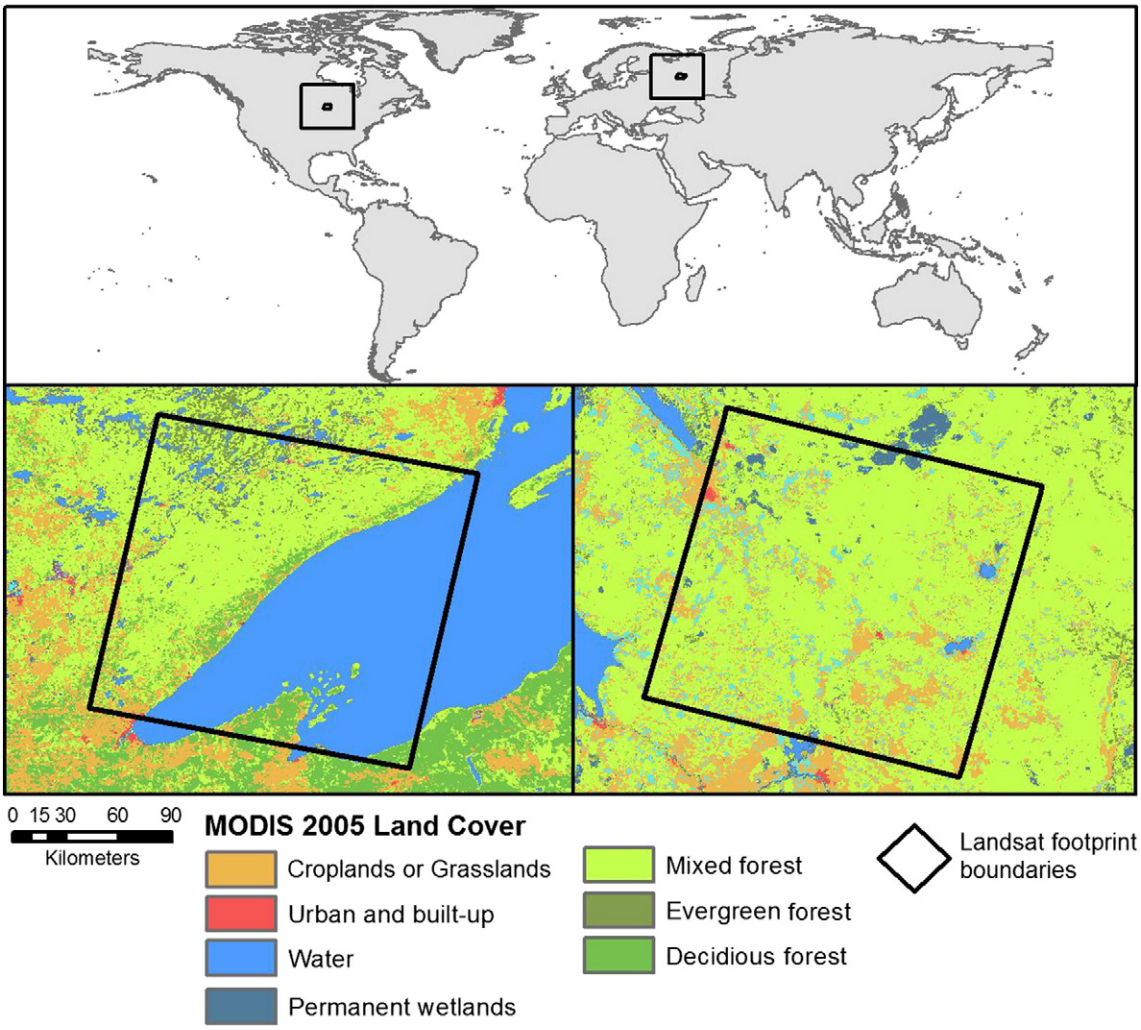

Fig. 1. Locations where the windfall classification method was tested. Study site 1 is located in the temperate zone of European Russia; study site 2 is located in the Greater Border Lake Region in northeast Minnesota (USA).

The index is an integrated Z-score depicting a pixel's probability of not being forest. Low IFI values indicate a higher likelihood of being forested areas and high IFI values a higher likelihood of other land cover classes (Huang et al., 2010). Using this information, we delineated "non-forest" pixels by applying a threshold. Huang et al. (2008) provides a more comprehensive explanation on how to choose and modify this threshold to capture pixels with low IFI values that are non-forest areas, such as dark green agricultural fields. We also collected less pure pixels at class boundaries for each category by adjusting the IFI threshold for a pixel being assigned to either forest or non-forest depending on whether their neighboring pixel was previously labeled as forest or non-forest (Huang et al., 2008).

Table 1
Image acquisition dates for the Landsat imagery used in this analysis. The images for footprint Path/Row 177/019 are ranked in the order they were used to create the image composite.

Path/Row 177/019			Path/Row 026/027		
Year in analysis	Acquisition date	Sensor	Year in analysis	Acquisition date	Sensor
2009	2009-07-11	TM5	1998	1998-09-16	TM5
	2009-08-23	ETM+			
	2009-07-30	TM5			
	2009-06-12	TM5			
	2009-05-19	TM5			
2011	2011-06-02	TM5	2000	2000-07-03	TM5
	2011-06-26	ETM+			
	2011-07-12	ETM+			
	2011-07-20	TM5			
	2011-05-25	ETM+			
	2011-08-05	TM5			

We used these training data in a Support Vector Machine (SVM) supervised classification. SVM are non-parametric classification algorithms that fit a linear hyperplane between two classes in a multi-dimensional space (Foody & Mathur, 2004a). Our strategy to collect training samples of both 'pure' forest pixels and 'less pure' forest pixels (as well as non-forest pixels) favored the application of SVM, because the linear separation between classes is strongly dependent on pixels along class boundaries (Foody & Mathur, 2004b). SVM use kernel functions to find the best fitting hyperplane, which require setting a kernel parameter for the kernel width ( ) and a regulation parameter (C). We chose the best parameter combination by comparing models that used a wide range of parameter combination and chose the parameters from the best fitting model (Janz, van der Linden, Waske, & Hostert, 2007).

2.4. Forest disturbance detection

We mapped forest disturbance in both locations using the Disturbance Index. The DI is a linear combination of normalized Tasseled-

Cap bands. The idea behind the index is that disturbance sites exhibit higher brightness, and lower greenness and wetness values compared to undisturbed forests. The Disturbance Index is calculated as:

$$DI = B_r - (G_r + W_r), \quad (2)$$

where B_r,G_r,W_r are the Tasseled Cap bands, standardized around the scene's mean forest value. Positive values generally indicate disturbance areas (Healey et al., 2005). The advantage of the Disturbance Index is that it only requires setting a threshold, which is typically study region dependent. For the Russia site, we visually compared the results of multiple thresholds against sample sites of stand-replacing disturbance as well as windfall sites and identified DI = 3.0 as providing the most accurate disturbance map. The same type of assessment for the U.S. site revealed that DI = 2.5 identified disturbed areas best. In the final step we combined the initial forest/non-forest map with the areas of forest disturbance and created a change-map for 2009–2011 and 1998–2000, respectively. We then applied a majority filter and defined a minimum mapping unit of 5 pixels (roughly equivalent to 0.5 ha) to eliminate isolated pixels that likely represented misclassifications.

2.5. Detecting windfall disturbance

Our windfall detection method was based on the assumption that only two forms of disturbances occurred on the landscape: windfall and harvests. To extract training data for each disturbance type, we visually examined the Landsat imagery to determine how wind-related disturbance may be spectrally different from clear-cut harvests. Based on these observations we postulated that, compared to harvests, a wind-related disturbance site would have:

(a) *Lower Tasseled Cap brightness values*: The Tasseled Cap brightness is a measure of the soil proportion in the signal and sensitive to the abundance of shadows (Kauth & Thomas, 1976). After a recent clear-cut harvest soil is often exposed and shadows are rare, leading to high brightness values. In contrast, after a windfall event, biomass often remains, reducing soil reflectance and maintaining shadows. This would result in lower brightness values for windfall disturbance than clear-cut harvests.

(b) *Higher Tasseled Cap wetness values*: The Tasseled Cap wetness provides information about the moisture content of a site (Cohen & Spies, 1992; Jin & Sader, 2005). Major over- and understory removal, typical for a clear-cut harvest, strongly reduces Tasseled Cap wetness (Ballard, 2000; Cohen & Goward, 2004; Healey et al., 2005). Hence, a windfall disturbance will have on average a higher Tasseled Cap wetness value than a clear-cut harvest.

(c) *Lower short-wave infrared (SWIR) reflectance (Landsat band 5)*: Similar to the Tasseled Cap wetness index, TM band 5 is sensitive to the amount of water in vegetation, but through an inverse relationship (Schroeder et al., 2011). On average, a windfall disturbance site would be expected to have lower SWIR then a clear-cut harvest due largely to more shadows in a windfall site.

Using normalized pixel values around a mean of zero following a standard Z-transformation, a histogram of all disturbed pixels will exhibit three main 'areas'. For example, in the case of band-5 reflectance, the locations of importance in the histogram are 1) the center, in which the spectral characteristics of windfall disturbance and clear cuts are essentially the same; 2) the left side of the histogram, which is dominated by 'windfall' pixels; and 3) the right side of the histogram, which is dominated by 'clear-cut harvest' pixels (Fig. 2). The nature of a normal distribution makes it convenient to target these areas. Specifically, we targeted areas to the left ('windfall') and to the right ('clear-cut') of one standard deviation from the mean, and extracted pixels located in these areas as training data for the 'windfall' and 'clear-cut harvest' categories. We then used the SVM to classify the disturbed areas, using the six multi-spectral bands from Landsat and the same parameter-search method as for the initial forest/non-forest classification.

In doing so, we were able to add information to our forest-change maps by attributing the cause of the forest disturbance. We postulated that a given cluster of disturbed pixels would have all been disturbed due the same cause, which especially in the case of windfall sites was confirmed during the validation process. Accordingly, we extracted all disturbance-labeled areas from our forest change map and converted these into vector-based polygons. These polygons were overlaid with our windfall classification map. Within each disturbance polygon, we then counted the number of pixels of each class (i.e., 'windfall' vs. 'clear-cut harvest') and assigned the final class label for the polygon based on the majority of the pixels in it.

2.6. Accuracy assessment

We assessed the accuracy of our methodology by evaluating (a) the accuracy of our forest-change map, and (b) the accuracy of windfall disturbance detection. For the forest-cover change maps, we randomly sampled 100 points from each of the three classes (i.e., 'constant forest', 'constant other', and 'disturbed'), and labeled each point manually using the Landsat composites and, where available, high-resolution imagery in Google-Earth. We then summarized the results in an error matrix, and calculated overall accuracy and the kappa statistics of the overall classification, as well as user's and producer's accuracy for each class (Congalton, 1991; Foody, 2002). To account for the possible sampling bias in the accuracy assessment, we area-weighted our classification accuracies (Card, 1982) and adjusted the area estimates of our categories (Stehman, 2012).

To estimate the performance of our proposed method in separating windfall from clear-cut harvests, we evaluated all disturbance sites to see whether or not they were assigned correctly to their expected class by visually inspecting the Landsat imagery and high-resolution Quickbird data. This analysis was supplemented with the following external datasets: for the Russia site, we had access to a hand-digitized validation dataset from 2010 from collaborators in the region. For the U.S. site, we used (a) a previously published Landsat-based classification of the region, which highlighted areas of windfall, fire, and logging disturbance (Wolter et al., 2012), and (b) a disturbance severity map created from IKONOS data (Rich et al., 2010). Both ancillary datasets did not cover our entire study region, but only areas in the northern half of the analyzed footprint (Wolter et al., 2012) and in the northwest of our study area (~121 km^2, Rich et al., 2010). We again generated an error-matrix to evaluate the accuracy of the classification of the polygons into 'windfall' and 'clear-cut harvest', and calculated the same accuracy measures.

3. Results

The forest change maps had high accuracies (Overall Accuracy 90.96% and Kappa value of 0.91 for the Russia change map; overall accuracy 89.33% and Kappa value of 0.84 for the U.S. site). User's and producer's accuracies were higher for the stable classes compared to the disturbance class and higher at the Russia site compared to the U.S. site (Table 2). The accuracy for the windfall classification was 77.5% for the Russia site and 76.4% for the U.S. site. In both cases, commission errors for 'windfall' category were slightly higher than those for 'clear-cut harvest' (Table 3).

At the Russia site, 68.5% of the landscape (over 23,000 km^2) was classified as forest in 2009. By 2011, 475 km^2 of the forested area experienced a form of disturbance, corresponding to an annual change rate of about 1%. Of the 475 km^2 of affected forest area, over 300 km^2 (or 64%) were caused by two large windfall events in 2009 and 2010. Overall, we analyzed 7,028 disturbance polygons in Russia, 4,625 (or 65.8%) of which were characterized as 'windfall'.

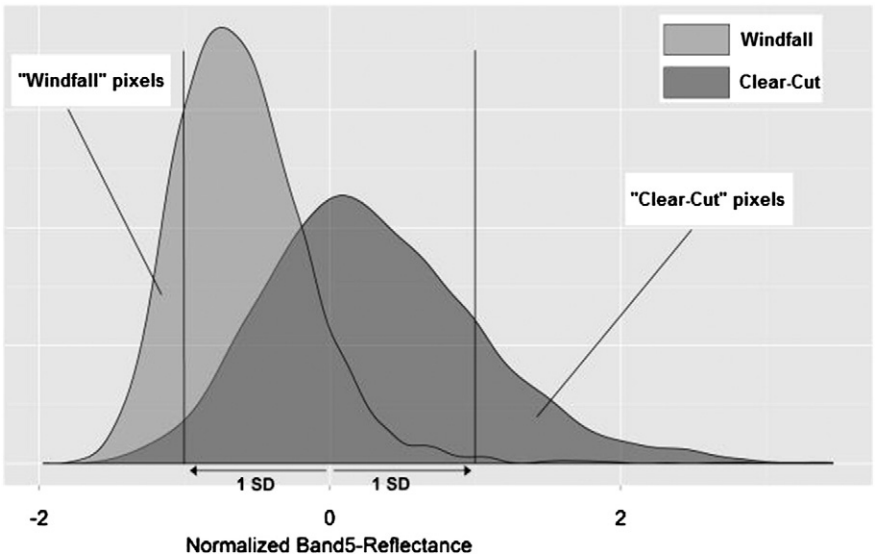

Fig. 2. Schematic representation training data collection strategy for the windfall classification. The data in the histogram represent values of the validation data of the Russian study site for the band-5 reflectance.

For the U.S. site, results were similar: in 1998, over 76% of the investigated area was forested (nearly 13,000 km^2). By 2000, 395 km^2 were disturbed, corresponding to an annual disturbance rate of 1.5%. Roughly 171 km^2, or 43%, of the affected area was damaged by wind. Overall, we analyzed 5,977 unique disturbance polygons at the U.S. site, of which 3,735 (or 63%) were caused by a large storm in 1999 (Fig. 3).

The point cloud featured two clusters, each of which contained observations of one disturbance type with very little ambiguity (i.e., 'windfall' or 'clear-cut harvest', Fig. 4). Between the two study sites, the point cloud of the U.S. site exhibited a larger difference between the two disturbance types.

The classification accuracy of the disturbance polygons also varied by size. At the Russian site (Fig. 5 top row) the lowest overall accuracy (just over 75%) was associated with the smallest disturbance polygons and then increased to an average of about 85% for disturbances of about 10 ha in size. After that size, the low number of polygons in each 0.5 ha-bin caused the data points containing to high variances to estimate a clear trend (Fig. 5a). For windfall sites only, small disturbance sites were more accurately detected than larger ones. The accuracy for windfall sites dropped from on average 95% for small patches to 80% for patches of about 8 ha in size. Again, for patch sizes larger than 8 ha the number of polygons became too small to estimate a clear trend (Fig. 5b). For clear-cut patches the classification accuracy was lowest (~55%) for the smallest patches close to our minimum mapping unit of 0.5 ha, but registered greater than 80% for patches of about 8 ha. For patches larger than 8 ha no clear trend was observable due to the low number of large disturbance patches (Fig. 5c). At the U.S. study site the general patterns of accuracy were very similar to the Russia site (Fig. 5d, e, f): For both disturbance types together, we found an increase in the classification accuracy from 70% for patches of 0.5 ha to over 95% for patches of about 7.5 ha in size (Fig. 5d). For windfall disturbances, accuracies were high throughout the entire range of disturbance patches: they were highest for the smallest and the largest windfalls (>95%) but slightly lower for windfalls of about 7–8 ha in size (~95%, Fig. 5e). However, here the trend was consistent across the entire range of patch sizes. For the clear-cut sites, the least accurate detection occurred for patches that were close to our minimum mapping unit of 0.5 ha. From there, the detection accuracy greatly improved with increasing patch size, yielding accuracies at about 80% for patches of about 5 ha in size (Fig. 5f).

At the Russia site we also noticed that the first major windfall event was classified at a higher accuracy compared to the second one (Fig. 6). Evaluating the spectral characteristics of these areas, we found that their band 5 reflectance values and Tasseled Cap brightness values were above zero while their Tasseled Cap wetness values were below zero.

4. Discussion

We developed a novel algorithm to separate windfall disturbance from harvested areas based on Landsat data and tested the method successfully in two different locations — one in the temperate zone of European Russia and one in the southern boreal forests of the United States. The generation of the forest disturbance map applied previously published methods to detect forest disturbances. Using this disturbance map, we then developed and applied a rule set that determined whether the disturbance was caused by windfall or a harvest event. To our knowledge this is the first study that developed a method specifically for the purpose of separating windfall disturbance from clear-cut harvesting and tested its robustness in multiple study regions.

Our results showed that in both study sites the separation between windfall and clear-cut disturbance was possible in over 75% of the disturbed area. Given the small number of studies that simultaneously classify windfall and clear-cut harvests using Landsat data, only a limited comparison to previous work can be made. Compared to the studies

Table 2
Area-weighted classification accuracies for our Landsat-based change-maps. Presented are the overall accuracies, kappa, user's and producer's accuracies for the three classes 'Constant Forest (F)', 'Constant Non-Forest (NF)' and 'Disturbance (D)'.

Landsat Path/Row	Overall accuracy [%]	Kappa	User's accuracy [%]			Producer's accuracy [%]		
			F	NF	D	F	NF	D
177019	90.96	0.91	91.00	91.00	88.00	95.40	84.07	66.28
026027	89.33	0.84	88.00	88.00	92.00	95.88	77.14	33.35

Table 3
Accuracy measures for the separation of the disturbance polygons into 'windfall' (W) and 'clear-cut harvest' (CC). Presented are the overall accuracy, the kappa statistics as well as user's and producer's accuracy.

Landsat Path/Row	Overall accuracy [%]	Kappa	User's accuracy [%]		Producer's accuracy [%]	
			W	CC	W	CC
177019	77.52	0.55	71.87	87.34	90.80	64.11
026027	76.39	0.55	62.95	98.80	98.86	61.54

of fire disturbance and clear-cut harvests (e.g., Pereira & Setzer, 1993; Roder et al., 2008; Schroeder et al., 2011), our accuracies were generally lower. For example, Schroeder et al. (2011) achieved classification accuracies greater than 90%, while our results suggest a little over 75% success rate when detecting windfall. We believe that two major factors contribute to these differences. The first factor is related to the difference in the methods of the two studies. Contrary to our study Schroeder et al. (2011) gathered training data with considerable user input. In contrast, our algorithm did not require any user intervention during the training process. Compared to classifications that gather training data manually, automated methods often yield lower classification accuracies. As such, the automation inherent in our algorithm is probably more prone to errors but comes with the advantage of not requiring manually collected training data. The second reason is related to forest management practices, particularly partial harvests. Partial harvests typically remove mature trees from the canopy while leaving younger trees uncut (Wilson & Sader, 2002), a management practice that is increasingly common particularly at the U.S. site. Partial harvests are known to impact Landsat's SWIR band (Olsson, 1994), a band that was highly important also in detecting windfall in our study. As such, it is possible that confusions between windfall and selective harvest lowered the overall detection accuracy, specifically by increasing the commission errors in our 'windfall' class. This highlights the need for a thorough understanding of harvesting practices before attributing disturbance types.

Our algorithm complements other efforts to process Landsat data with little or no user input (Healey et al., 2005; Huang et al., 2010). In the present study, we integrated two basic concepts that had not been previously combined to produce a forest-cover change map: the dark-object concept (Huang et al., 2008), and the Disturbance Index concept (Healey et al., 2005). Our disturbance attribution step was then based on the disturbance areas in the change map. We therefore stress that the attribution step, itself, can be combined with any other algorithm that detects forest disturbance using Landsat images.

Overall, the combination of the selected variables proved to be suitable in separating windfall disturbance from clear-cuts. Previous work on forest change detection suggests that both Landsat SWIR reflectance (band 5) and Tasseled Cap wetness values (a contrast of SWIR with the visible and near infrared bands) contain similar levels of information (Chen & Vierling, 2006; Cohen & Goward, 2004; Healey et al., 2005; Peddle, Hall, & LeDrew, 1999; Schroeder et al., 2011). Similarly, SWIR and the Tasseled Cap brightness often show a high degree of correlation (Cohen, Maiersperger, Gower, & Turner, 2003). However, initial tests using all permutations of the three bands during the training data collection suggested that the highest classification accuracy was achieved by using all three bands as opposed to using one band individually or in combination with another band. This might suggest that although correlated, each band contributes a unique source of information about windfall and harvest sites, so we suggest that even correlated information can be useful for improving classification accuracies.

Our results also suggest that the accuracy of the disturbance type classification increased with the size of a disturbed area. This size-

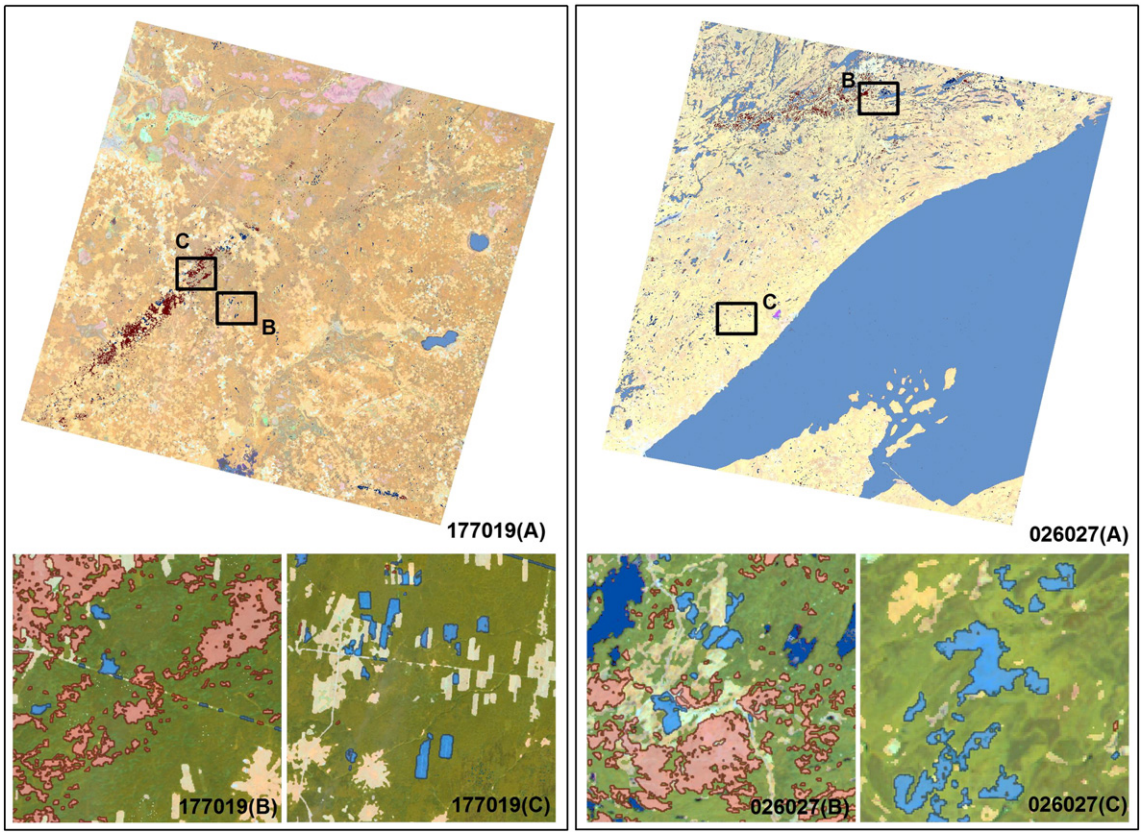

Fig. 3. Classification results for the Russia site (left) and the U.S. site (right). For both study locations, examples are presented of areas characterized primarily by windfall disturbance (177019A and 026027A), and areas primarily characterized by clear-cut harvest (177019B and 026027B).

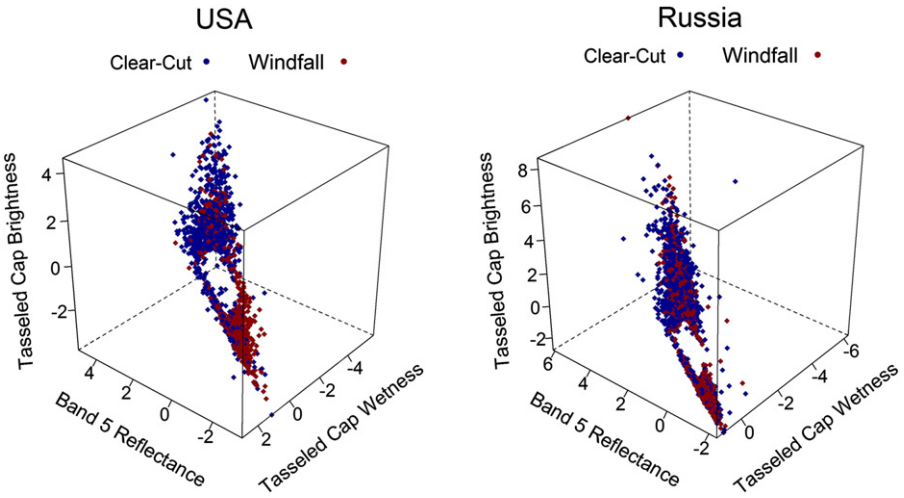

Fig. 4. Validation of the training data to classify disturbance areas into 'windfall' and 'clear-cut harvest' in the spectral feature space in which they were generated.

related classification accuracy issue is potentially an artifact due to two aspects of our study design. First, mixed pixels along edges affect a small disturbance site more strongly than a larger site. Second, the generalization of disturbance sites at the polygon-level, posterior to the classification, may have introduced errors. Our decision to use the majority rule prior to delineating disturbance polygons might have affected particularly long and narrow disturbed patches. Despite these shortcomings, our algorithm represents a valuable contribution to forest disturbance mapping. Overall, we achieved mean classification accuracies of over 75%, and even higher values for larger disturbance patches. This suggests that for the vast majority of the disturbance area (83.3% at the Russia site, and 87.5% at the U.S. site), the classification results identified the main events that took place on the ground, i.e., widespread windfalls, correctly.

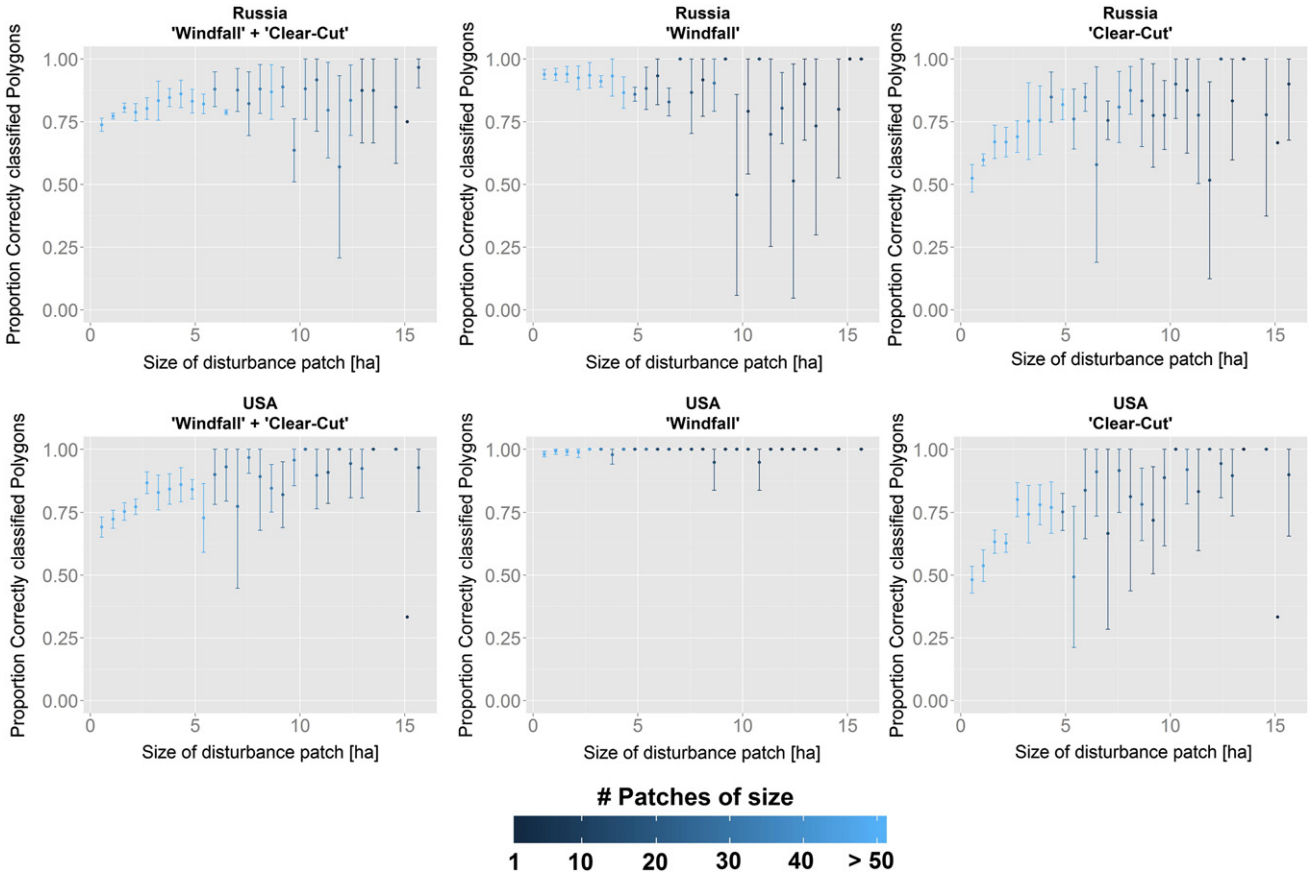

Fig. 5. Proportion of correctly classified disturbance patches by patch size for the two classes, 'windfall' and 'clear-cut harvest', and the two classes combined. The top row represents the Russian site (footprint 177019), the bottom row the U.S. site (footprint 026027). The data presented are binned data with a bin width of 0.5 ha. Every bin was subdivided into six groups with 0.09 ha increments in patch size (i.e., increments of one Landsat pixel). The point represent the mean proportion correctly classified polygons across sub-groups in each bin, the error bars represent the standard deviation. The colors represent the number of polygons in every bin.

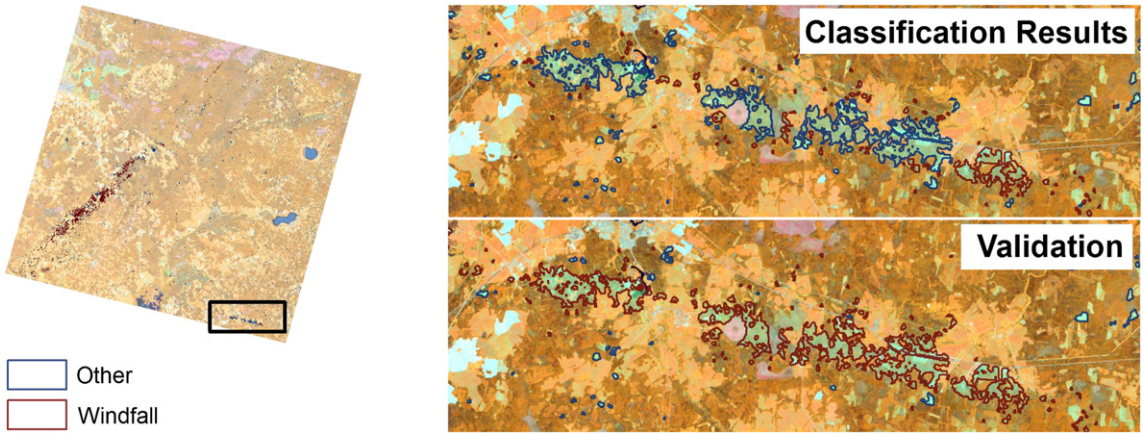

Fig. 6. Misclassified disturbance site. Classification results suggest that the disturbance is caused by harvest. Validation data reveal that the site is caused by windfall.

A number of uncertainties also remain. First, the windfall detection algorithm requires knowledge about a windfall event in the region of interest. Second, we were not able to test how the presence of fire or insect defoliation would affect our results. We can only speculate that a step-wise approach and the addition of fire-specific indices such as the Normalized Burn Ratio (NBR) could help isolate fire-affected pixel, which then could be used to sample training data. Third, we did not distinguish between different levels of windfall severity, which will likely impact the spectral signal (Rich et al., 2010). Fourth, the image composites at the Russian site might have introduced errors across the landscapes because of the different phenological stages. Though, the critical image dates (e.g., the May imagery) only covered a small proportion of the landscape and acquired climate records indicated that these errors were assumingly small. Fifth, we did not test how varying the threshold (i.e., we used one standard deviation away from the mean) of collecting windfall and clear-cut training data in the histogram would have affected our results, but we suspect that the threshold is sensitive to the proportion of 'windfall' and 'clear-cut' disturbance in the classification. Finally, at the Russia site, a second major windfall was largely missed by our algorithms (Fig. 6). While not having complete evidence due to missing ancillary information, two reasons potentially contribute to this omission. First, the 2010 storm event may have been a much stronger one compared to the 2009 event, causing more biomass to be removed from the site, making it spectrally more similar to a clear-cut harvest. The second, and in our opinion more likely, reason is salvage logging following the windfall. During salvage logging the damaged trees are removed from the site, rendering it spectrally similar to a clear-cut harvest. As such, the post-storm treatment of a site is a major factor impacting the correct classification of windfall disturbance using satellite imagery.

Knowing what caused a forest disturbance is valuable information for a variety of research questions that utilize forest disturbance maps. While the literature on remote sensing of fire- and insect-related disturbance is fairly rich, work on identifying windfall disturbance has not received much attention. Here, we developed a novel algorithm to generate training data and classify disturbance areas into 'windfall' and 'clear-cut harvest' disturbances. Our methodology requires minimal user input, and can be immediately applied to other Landsat based disturbance maps. The proposed method resulted in good classification accuracies, was effective in separating windfall and clear-cut harvest, and maintained similar accuracies across two different study regions. As with any other form of classification, the increased level of categorical information produced as a result of this work is of great value, especially for research that require information about changes in forest areas, such as econometric analyses that assess drivers of timber harvest and carbon management.

Acknowledgements

We gratefully acknowledge the support by the Land-Cover and Land-Use Change (LCLUC) Program of the National Aeronautic Space Administration (NASA) through grant NNX08AK77G. We are thankful for data support by collaborators from Greenpeace Russia. We also would like to thank the anonymous reviewers for the comments, which greatly helped improving the manuscript.

References

Achard, F., Eva, H. D., Stibig, H. J., Mayaux, P., Gallego, J., Richards, T., et al. (2002). Determination of deforestation rates of the world's humid tropical forests. *Science*, *297*, 999–1002.

Achard, F., Mollicone, D., Stibig, H. J., Aksenov, D., Laestadius, L., Li, Z. Y., et al. (2006). Areas of rapid forest-cover change in boreal Eurasia. *Forest Ecology and Management*, *237*, 322–334.

Andam, K. S., Ferraro, P. J., Pfaff, A., Sanchez-Azofeifa, G. A., & Robalino, J. A. (2008). Measuring the effectiveness of protected area networks in reducing deforestation. *Proceedings of the National Academy of Sciences of the United States of America*, *105*, 16089–16094.

Ballard, T. M. (2000). Impacts of forest management on northern forest soils. *Forest Ecology and Management*, *133*, 37–42.

Baumann, M., Ozdogan, M., Kuemmerle, T., Wendland, K. J., Esipova, E., & Radeloff, V. C. (2012). Using the Landsat record to detect forest-cover changes during and after the collapse of the Soviet Union in the temperate zone of European Russia. *Remote Sensing of Environment*, *124*, 174–184.

Bonan, G. B. (2008). Forests and climate change: Forcings, feedbacks, and the climate benefits of forests. *Science*, *320*, 1444–1449.

Card, D. H. (1982). Using known map category marginal frequencies to improve estimates of thematic map accuracy. *Photogrammetric Engineering and Remote Sensing*, *48*, 431–439.

Chen, X. X., & Vierling, L. (2006). Spectral mixture analyses of hyperspectral data acquired using a tethered balloon. *Remote Sensing of Environment*, *103*, 338–350.

Cheung, H. F., Pan, J. Y., Gu, Y. Z., & Wang, Z. Z. (2013). Remote-sensing observation of ocean responses to Typhoon Lupit in the northwest Pacific. *International Journal of Remote Sensing*, *34*, 1478–1491.

Chomitz, K. M., & Gray, D. A. (1996). Roads, land use, and deforestation: A spatial model applied to Belize. *World Bank Economic Review*, *10*(3), 487–512.

Cohen, W. B., Fiorella, M., Gray, J., Helmer, E., & Anderson, K. (1998). An efficient and accurate method for mapping forest clearcuts in the Pacific Northwest using Landsat imagery. *Photogrammetric Engineering and Remote Sensing*, *64*, 293–300.

Cohen, W. B., & Goward, S. A. (2004). Landsat's role in ecological applications of remote sensing. *BioScience*, *54*(6), 535–545.

Cohen, W. B., Maiersperger, T. K., Gower, S. T., & Turner, D. P. (2003). An improved strategy for regression of biophysical variables and Landsat ETM + data. *Remote Sensing of Environment*, *84*, 561–571.

Cohen, W. B., & Spies, T. A. (1992). Estimating structural attributes of Douglas-fir/western hemlock forest stands from landsat and SPOT imagery. *Remote Sensing of Environment*, *41*, 1–17.

Congalton, R. G. (1991). A review of assessing the accuracy of classifications of remotely sensed data. *Remote Sensing of Environment*, *37*, 35–46.

Coppin, P. R., & Bauer, M. E. (1994). Processing of multitemporal Landsat TM imagery to optimize extraction of forest-cover change features. *IEEE Transactions on Geoscience and Remote Sensing*, *32*, 918–927.

Crist, E. P., & Kauth, R. J. (1986). The Tasseled Cap de-mystified. *Photogrammetric Engineering and Remote Sensing*, *52*, 81–86.

FAO (2005). Global forest resource assessment 2005. In FAO (Ed.), *Forestry Papers*. Rome, Italy: Food and Agriculture Organization of the United Nations.

FAO (2010). In Food and Agriculture Organization of the United Nations (Ed.), *Global forest resource assessment 2010* (pp. 378).
Foody, G. M. (2002). Status of land cover classification accuracy assessment. *Remote Sensing of Environment*, *80*, 185–201.
Foody, G. M., & Mathur, A. (2004). A relative evaluation of multiclass image classification by support vector machines. *IEEE Transactions on Geoscience and Remote Sensing*, *42*, 1335–1343.
Foody, G. M., & Mathur, A. (2004). Toward intelligent training of supervised image classifications: Directing training data acquisition for SVM classification. *Remote Sensing of Environment*, *93*, 107–117.
Frelich, L. E., & Reich, P. B. (1995). Spatial patterns and succession in a Minnesota southern-boreal forest. *Ecological Monographs*, *65*, 325–346.
French, N. H. F., Kasischke, E. S., Hall, R. J., Murphy, K. A., Verbyla, D. L., Hoy, E. E., et al. (2008). Using Landsat data to assess fire and burn severity in the North American boreal forest region: An overview and summary of results. *International Journal of Wildland Fire*, *17*, 443–462.
Garcia-Haro, F. J., Gilabert, M.A., & Melia, J. (2001). Monitoring fire-affected areas using Thematic Mapper data. *International Journal of Remote Sensing*, *22*, 533–549.
Gorsevski, V., Kasischke, E., Dempewolf, J., Loboda, T., & Grossmann, F. (2012). Analysis of the Impacts of armed conflict on the Eastern Afromontane forest region on the South Sudan–Uganda border using multitemporal Landsat imagery. *Remote Sensing of Environment*, *118*, 10–20.
Hansen, M. C., & DeFries, R. S. (2004). Detecting long-term global forest change using continuous fields of tree-cover maps from 8-km advanced very high resolution radiometer (AVHRR) data for the years 1982–99. *Ecosystems*, *7*, 695–716.
Hansen, M., DeFries, R., Townshend, J. R., Carroll, M., Dimiceli, C., & Sohlberg, R. (2006). *Vegetation continuous fields MOD44B, 2001 percent tree cover, Collection 4.* College Park, Maryland: University of Maryland (2001).
Hansen, M. C., Stehman, S. V., & Potapov, P. V. (2010). Quantification of global gross forest cover loss. *Proceedings of the National Academy of Sciences*, *107*, 8650–8655.
Hayes, T. M. (2006). Parks, people, and forest protection: An institutional assessment of the effectiveness of protected areas. *World Development*, *34*, 2064–2075.
He, L. M., Chen, J. M., Zhang, S. L., Gomez, G., Pan, Y. D., McCullough, K., et al. (2011). Normalized algorithm for mapping and dating forest disturbances and regrowth for the United States. *International Journal of Applied Earth Observation and Geoinformation*, *13*, 236–245.
Healey, S. P., Cohen, W. B., Yang, Z. Q., & Krankina, O. N. (2005). Comparison of Tasseled Cap-based Landsat data structures for use in forest disturbance detection. *Remote Sensing of Environment*, *97*, 301–310.
Hicke, J. A., Allen, C. D., Desai, A.R., Dietze, M. C., Hall, R. J., Hogg, E. H., et al. (2012). Effects of biotic disturbances on forest carbon cycling in the United States and Canada. *Global Change Biology*, *18*, 7–34.
Huang, C., Goward, S. N., Masek, J. G., Thomas, N., Zhu, Z., & Vogelmann, J. E. (2010). An automated approach for reconstructing recent forest disturbance history using dense Landsat time series stacks. *Remote Sensing of Environment*, *114*, 183–198.
Huang, C. Q., Song, K., Kim, S., Townshend, J. R. G., Davis, P., Masek, J. G., et al. (2008). Use of a dark object concept and support vector machines to automate forest cover change analysis. *Remote Sensing of Environment*, *112*, 970–985.
Irons, J. R., Dwyer, J. L., & Barsi, J. A. (2012). The next Landsat satellite: The Landsat Data Continuity Mission. *Remote Sensing of Environment*, *122*, 11–21.
Janz, A., van der Linden, S., Waske, B., & Hostert, P. (2007). imageSVM — A user-orientated tool for advanced classification of hyperspectral data using Support Vector Machines. *Proceedings of the 5th EARSeL workshop on Imaging Spectroscopy, Bruges, Belgium*.
Jin, S., & Sader, S. A. (2005). Comparison of time series tasseled cap wetness and the normalized difference moisture index in detecting forest disturbances. *Remote Sensing of Environment*, *94*, 364–372.
Kasischke, E. S., Amiro, B.D., Barger, N. N., French, N. H. F., Goetz, S. J., Grosse, G., et al. (2013). Impacts of disturbance on the terrestrial carbon budget of North America. *Journal of Geophysical Research – Biogeosciences*, *118*, 303–316.
Kauth, R. J., & Thomas, G. S. (1976). The Tasselled Cap — A graphic description of the spectral-temporal development of agricultural crops as seen by LANDSAT. *LARS Symposia, Paper 159*.
Koroleva, N. V., & Ershov, D.V. (2012). Assessment of an error of determination of areas windfalls using space images of high spatial resolution of Landsat-TM (in Russian). *Actual problems in remote sensing of the Earth from Space. , 9.* (pp. 80–86).
Krylov, A. M., Malahova, E. G., & Vladimirova, N. A. (2012). Identification and assessment of forest areas damaged by windfalls in 2009–2010 by means of remote sensing (in Russian). *Proceedings of the St. Petersburg Forest Technical Academy*, *197–207*.
Masek, J. G., Cohen, W. B., Leckie, D., Wulder, M.A., Vargas, R., de Jong, B., et al. (2011). Recent rates of forest harvest and conversion in North America. *Journal of Geophysical Research – Biogeosciences*, *116*.
Masek, J. G., Huang, C., Wolfe, R., Cohen, W., Hall, F., Kutler, J., et al. (2008). North American forest disturbance mapped from a decadal Landsat record. *Remote Sensing of Environment*, *112*, 2914–2926.
Masek, J. G., Vermote, E. F., Saleous, N. E., Wolfe, R., Hall, F. G., Huemmrich, K. F., et al. (2006). A Landsat surface reflectance dataset for North America, 1990–2000. *IEEE Geoscience and Remote Sensing Letters*, *3*, 68–72.
Mutanen, A., & Toppinen, A. (2007). Price dynamics in the Russian-Finnish roundwood trade. *Scandinavian Journal of Forest Research*, *22*, 71–80.
Negron-Juarez, R., Baker, D. B., Zeng, H. C., Henkel, T. K., & Chambers, J. Q. (2010). Assessing hurricane-induced tree mortality in U.S. Gulf Coast forest ecosystems. *Journal of Geophysical Research – Biogeosciences*, *115*.
Nelson, B. W., Kapos, V., Adams, J. B., Wilson, J. O., & Braun, O. P. G. (1994). Forest disturbance by large blowdowns in the Brazilian Amazon. *Ecology*, *75*, 853–858.
Olsson, H. (1994). Changes in satellite-measured reflectances caused by thinning cuttings in Boreal forest. *Remote Sensing of Environment*, *50*, 221–230.
Ozdogan, M. (2014). *Automated forest disturbance mapping with Support Vector Machines and incomplete training data.* (in press).
Patterson, M. W., & Yool, S. R. (1998). Mapping fire-induced vegetation mortality using Landsat Thematic Mapper data: A comparison of linear transformation techniques. *Remote Sensing of Environment*, *65*, 132–142.
Peddle, D. R., Hall, F. G., & LeDrew, E. F. (1999). Spectral mixture analysis and geometric-optical reflectance modeling of boreal forest biophysical structure. *Remote Sensing of Environment*, *67*, 288–297.
Pereira, M. C., & Setzer, A. W. (1993). Spectral characteristics of fire scars in Landsat-5T images of Amazonia. *International Journal of Remote Sensing*, *14*, 2061–2078.
Peterson, C. J. (2000). Damage and recovery of tree species after two different tornadoes in the same old growth forest: A comparison of infrequent wind disturbances. *Forest Ecology and Management*, *135*, 237–252.
Potapov, P., Hansen, M. C., Stehman, S. V., Pittman, K., & Turubanova, S. (2009). Gross forest cover loss in temperate forests: Biome-wide monitoring results using MODIS and Landsat data. *Journal of Applied Remote Sensing*, *3*.
Potapov, P. V., Turubanova, S. A., Hansen, M. C., Adusei, B., Broich, M., Altstatt, A., et al. (2012). Quantifying forest cover loss in Democratic Republic of the Congo, 2000–2010, with Landsat ETM + data. *Remote Sensing of Environment*, *122*, 106–116.
Price, C., & Murphy, B. (2002). Lightning activity during the 1999 Superior Derecho. *Geophysical Research Letters*, *29*, 21–42.
Ramsey, E., Rangoonwala, A., Middleton, B., & Lu, Z. (2009). Satellite Optical and Radar used to track Wetland Forest impact and short-term recovery from Hurricane Katrina. *Wetlands*, *29*, 66–79.
Ramsey, E., Werle, D., Lu, Z., Rangoonwala, A., & Suzuoki, Y. (2009). A case of timely satellite image acquisitions in support of coastal emergency environmental response management. *Journal of Coastal Research*, *25*, 1168–1172.
Rich, R. L., Frelich, L., Reich, P. B., & Bauer, M. E. (2010). Detecting wind disturbance severity and canopy heterogeneity in boreal forest by coupling high-spatial resolution satellite imagery and field data. *Remote Sensing of Environment*, *114*, 299–308.
Roder, A., Hill, J., Duguy, B., Alloza, J. A., & Vallejo, R. (2008). Using long time series of Landsat data to monitor fire events and post-fire dynamics and identify driving õfactors. A case study in the Ayora region (eastern Spain). *Remote Sensing of Environment*, *112*, 259–273.
Scheller, R. M., & Mladenoff, D. J. (2004). A forest growth and biomass module for a landscape simulation model, LANDIS: Design, validation, and application. *Ecological Modelling*, *180*(1), 211–229.
Schroeder, T. A., Wulder, M.A., Healey, S. P., & Moisen, G. G. (2011). Mapping wildfire and clearcut harvest disturbances in boreal forests with Landsat time series data. *Remote Sensing of Environment*, *115*, 1421–1433.
Sieber, A., Kuemmerle, T., Prishchepov, A. V., Wendland, K. J., Baumann, M., Radeloff, V. C., Baskin, L. M., & Hostert, P. (2013). Landsat-based mapping of post-Soviet land-use change to assess the effectiveness of the Oksky and Mordovsky protected areas in European Russia. *Remote Sensing of Environment*, *133*, 38–51.
Stehman, S. V. (2012). Impact of sample size allocation when using stratified random sampling to estimate accuracy and area of land-cover change. *Remote Sensing Letters*, *3*, 111–120.
Townsend, P. A., Singh, A., Foster, J. R., Rehberg, N. J., Kingdon, C. C., Eshleman, K. N., et al. (2012). A general Landsat model to predict canopy defoliation in broadleaf deciduous forests. *Remote Sensing of Environment*, *119*, 255–265.
Van Wagtendonk, J. W., Root, R. R., & Key, C. H. (2004). Comparison of AVIRIS and Landsat ETM + detection capabilities for burn severity. *Remote Sensing of Environment*, *92*, 397–408.
Vogelmann, J. E., Tolk, B., & Zhu, Z. (2009). Monitoring forest changes in the southwestern United States using multitemporal Landsat data. *Remote Sensing of Environment*, *113*, 1739–1748.
Wang, F. G., & Xu, Y. J. (2010). Comparison of remote sensing change detection techniques for assessing hurricane damage to forests. *Environmental Monitoring and Assessment*, *162*, 311–326.
Webb, S. L., & Scanga, S. E. (2001). Windstorm disturbance without patch dynamics: Twelve years of change in a Minnesota forest. *Ecology*, *82*, 893–897.
Wendland, K. J., Baumann, M., Lewis, D. J., Sieber, A., & Radeloff, V. C. (2014). *Protected area effectiveness in European Russia during and after the collapse of the Soviet Union.* (in review).
Wendland, K. J., Lewis, D. J., Alix-Garcia, J., Ozdogan, M., Baumann, M., & Radeloff, V. C. (2011). Regional- and district-level drivers of timber harvesting in European Russia after the collapse of the Soviet Union. *Global Environmental Change*, *21*, 1290–1300.
Wilson, E. H., & Sader, S. A. (2002). Detection of forest harvest type using multiple dates of Landsat TM imagery. *Remote Sensing of Environment*, *80*, 385–396.
Wolter, P. T., Sturtevant, B. R., Miranda, B. R., Lietz, S. M., Townsend, P. A., & Pastor, J. (2012). *Forest land cover change (1975–2000) in the Greater Border Lakes region.* Research Map NRS-3. Newtown Square, PA: U.S. Department of Agriculture, Forest Service, Northern Research Station. http://dx.doi.org/10.2737/RDS-2012-0007 (17 pp.).
Wulder, M.A., Masek, J. G., Cohen, W. B., Loveland, T. R., & Woodcock, C. E. (2012). Opening the archive: How free data has enabled the science and monitoring promise of Landsat. *Remote Sensing of Environment*, *122*, 2–10.
Zhu, Z., & Woodcock, C. E. (2012). Object-based cloud and cloud shadow detection in Landsat imagery. *Remote Sensing of Environment*, *118*, 83–94.
Zhu, Z., Woodcock, C. E., & Olofsson, P. (2012). Continuous monitoring of forest disturbance using all available Landsat imagery. *Remote Sensing of Environment*, *122*, 75–91.